DOI: 10.24850/j-tyca-15-01-03

Articles

Impact of climate change on future discharges from a high Andean basin in Peru to 2100

Impacto del cambio climático en las descargas futuras de una cuenca altoandina de Perú al 2100

Sandra del Aguila[1], ORCID: https://orcid.org/0000-0001-8051-3575

Francisco Espinoza-Montes[2], ORCID: https://orcid.org/0000-0002-0093-7050

[1]National University of San Cristobal de Huamanga, Ayacucho, Peru, sandra.delaguila@unsch.edu.pe

[2]National University of the Center of Peru, Huancayo, Peru, franciscoespinozamontes@gmail.com

Corresponding author: Sandra del Aguila, sandra.delaguila@unsch.edu.pe

Abstract

The objective of this research was to analyze the impact of climate change on the behavior of monthly discharges in the Anya basin, a tributary of

the Mantaro, Junin, at 2100, with the SWAT (Soil and Water Assessment Tool) model. Daily gridded data on precipitation and temperatures were obtained from PISCO (Peruvian Interpolated data of the SENAMHI's Climatological and Hydrological Observations) between 1981 and 2015 and average monthly flows measured at the Anya hydrometric station. For the analysis of the space-time effect of climate change on temperature and precipitation and its influence on basin runoff, five global climate models (ACCES1.0, bcc_csm1, BNU_ESM, CMCC_CM and GISS_E2) were used in two emission scenarios (RCP 4.5 and 8.5). The simulation was carried out for the period 2070-2100, considering 1980-2010 as the base period. The model worked satisfactorily with the statistical values of Nash-Sutcliffe (NSE), PBIAS and coefficient of determination (R^2). In the basin, the average results show an increase in precipitation (between 4.63 and 8.14 %) and temperature (from 2.3 to 4.2 °C), in RCP 4.5 and 8.5 scenarios by 2100. Likewise, there would be an increase in flows in comparison with the base period, obtaining that, on average, the flow in the basin would increase by 2.4 and 12.6 % in the RCP 4.5 and 8.5 scenarios, respectively. It is concluded that the increase in temperature and precipitation will influence a greater runoff and risk of flooding in the cultivation areas in the basin.

Keywords: PISCO-SENAMHI, SWAT, global climate models (GCM), RCP scenarios.

Tecnología y Ciencias del Agua

OPEN ACCESS

Check for updates

Resumen

El objetivo de esta investigación fue analizar el impacto del cambio climático en el comportamiento de las descargas mensuales en la cuenca Anya, afluente del Mantaro, Junín, al 2100, con el modelo SWAT (Soil and Water Assessment Tool). Se obtuvieron datos grillados diarios de precipitación y temperaturas de PISCO (Peruvian Interpolated data of the SENAMHI's Climatological and Hydrological Observations) entre 1981 y 2015, y caudales promedio mensuales medidos en la estación hidrométrica Anya. Para el análisis del efecto espacio temporal del cambio climático en la temperatura y precipitación, y su influencia en el escurrimiento de la cuenca, se utilizaron cinco modelos climáticos globales (ACCES1.0, bcc_csm1, BNU_ESM, CMCC_CM y GISS_E2) en dos escenarios de emisiones (RCP 4.5 y 8.5). La simulación se realizó para el periodo 2070-2100, considerándose como periodo base 1980-2010. El modelo funcionó satisfactoriamente con los valores estadísticos de Nash-Sutcliffe (NSE), PBIAS y coeficiente de determinación (R^2). En la cuenca, los resultados promedio muestran un incremento de precipitación (entre 4.63 y 8.14 %) y temperatura (de 2.3 a 4.2 °C), en escenarios RCP 4.5 y 8.5 al 2100. Asimismo, habría un incremento de caudales en comparación con el periodo base, obteniéndose que, en promedio, el caudal en la cuenca aumentaría en 2.4 y 12.6 % en los escenarios RCP 4.5 y 8.5, respectivamente. Se concluye que el incremento de temperatura y precipitación influirá en una mayor escorrentía y riesgo de inundaciones en las áreas de cultivo en la cuenca.

Palabras clave: PISCO-SENAMHI, SWAT, modelos climáticos globales (MCGs), escenarios RCP.

Received: 28/02/2022

Accepted: 06/06/2022

Published online: 15/07/2022

Introduction

Issues related to water resources are widely disseminated and discussed throughout the world because they are essential for life on the planet; therefore, studies to evaluate its distribution in time and space are of the utmost importance (Almeida, Pereira, & Pinto, 2018). In that sense, the application of hydrological models for rainfall-runoff simulation and flood prediction has received great attention in recent years and numerous research studies have been carried out in these fields (Nazari, Masoud, & Karakouzian, 2020). Hydrological models seek to capture the physical mechanisms of generation of surface runoff and recharge of underground aquifers from precipitation and evapotranspiration (Ocampo & Velez, 2013).

Knowing and identifying the predominant processes in the basins allow the management and planning of water resources with the aim of predicting the hydrological behavior of a basin in different climate scenarios, allowing the development of effective management strategies

(Ashu & Lee, 2020). This requires analyzing the risk of water scarcity, forced by changing climate, land use alterations, population growth and industrialization to pave the way for sustainable planning and management of water resource systems (Swain, Mishra, Sahoo, & Chatterjee, 2020). Likewise, the change of land use [coverage] influences ecosystems, causing transformations in the rate of provision of water ecosystem services, assuming an important role in the hydrological cycle, since, for example, the evapotranspiration process depends on the type of cover, climate and available water capacity for plants, in addition to increasing surface runoff or attenuating it (González-Celada, Ríos, Benegas-Negri, & Argotty-Benavides, 2021).

Currently there are many hydrological models that allow simulating the discharge of rivers with greater precision, ease and speed than the traditional measurement method. Among them is the SWAT model, which is a basin-scale model integrated with ArcGIS, to help improve the accuracy of the simulated rainfall-runoff result using the physical properties of the basin (Asurza & Lavado, 2020). Understanding the hydrological processes within a basin is essential for better management of water resources, which is why SWAT, internationally accepted as a robust tool for interdisciplinary modeling of water resources, was applied in this study (Abbaspour, Vaghefi, & Srinivasan, 2017). The SWAT semi-distributed hydrological model has been successfully applied to simulate seasonal and polluting water in agricultural watersheds and its uses have been successfully calibrated and validated in many regions around the world (Gomáriz & Sarría, 2018; Deng, Pisani, Hernández, & Li, 2020). Additionally, SWAT has the ability to incorporate weather anomalies and

coverage changes into the simulation process (Neitsch, Arnold, Kiniry, Williams, & King, 2005).

The impact of climate change is assessed using global climate models (GCMs) from Phase 5 of the Coupled Model Intercomparison Project (CMIP5) (Taylor, Stouffer, & Meehl, 2012) which brings together a variety of GCMs that have grown in complexity over time, improving the representation of the processes and incorporating new uncertainties associated with the different parameterizations. However, they still present a certain dispersion between them and in the definition of some variables (Penalba & Pántano, 2019). Several studies have focused on the possible impacts of climate change on water resources (Molina-Navarro *et al*., 2016; Deng *et al*., 2020) testing different emission scenarios (for example, RCP 4.5 and RCP 8.5). Agricultural activity is directly related to water resources and food security, therefore, climate change has direct and indirect effects on food production due to temperature changes, irregular rainfall and the occurrence of extreme weather events (Wongchuig, Mello, & Chou, 2018).

The study basin is located in the central Andes of Peru and its runoff contributes to the flow of the Mantaro River, where 71 % of agricultural areas receive water exclusively from rain (IGP, 2005). In addition, the agricultural production of the Mantaro river basin supplies the capital city of Lima and is the basin with the highest population density in the Peruvian mountainous regions (Wongchuig *et al*., 2018).

Based on the above, the objective of this research was to carry out hydrological modeling and simulation of monthly discharges with SWAT,

using variations in precipitation and temperature extracted from global climate models (GCMs) in two emission scenarios - RCP 4.5 and RCP 8.5 for the period 2070-2100 (taking 1980-2010 as the base period), in order to analyze the impact of climate change on monthly discharges in the future.

Materials and methods

Study area

The Anya river basin is located in the central high Andean zone of Peru, located on the left bank of the Mantaro river between 11.98° to 11.89° south latitude and 75.28° to 75.21° west longitude (Figure 1). Its drainage area is 48.03 km2, however, the area up to the gauging point is 41.7 km2, the length of the main course is 11.3 km with an average annual flow of 0.51 m3/s; its average altitude is 3700 meters above sea level with a slope of 20.9 %. The multiannual average precipitation is approximately 800 mm and has a seasonal behavior where 84 % falls between September and March, with sporadic rains in April and May, being nil between June and August. The predominant life zone according to the Holdridge life zone classification system (Sabino, Lavado, & Aybar, 2019) is the Tropical Low Montane Dry Forest (df-TLM) occupying 65.22 % of the basin area; said predominance corresponds to the amount of precipitation. The climate in the area is varied due to the diversity of

altitudinal floors, however, on average, it corresponds to a cold temperate climate.

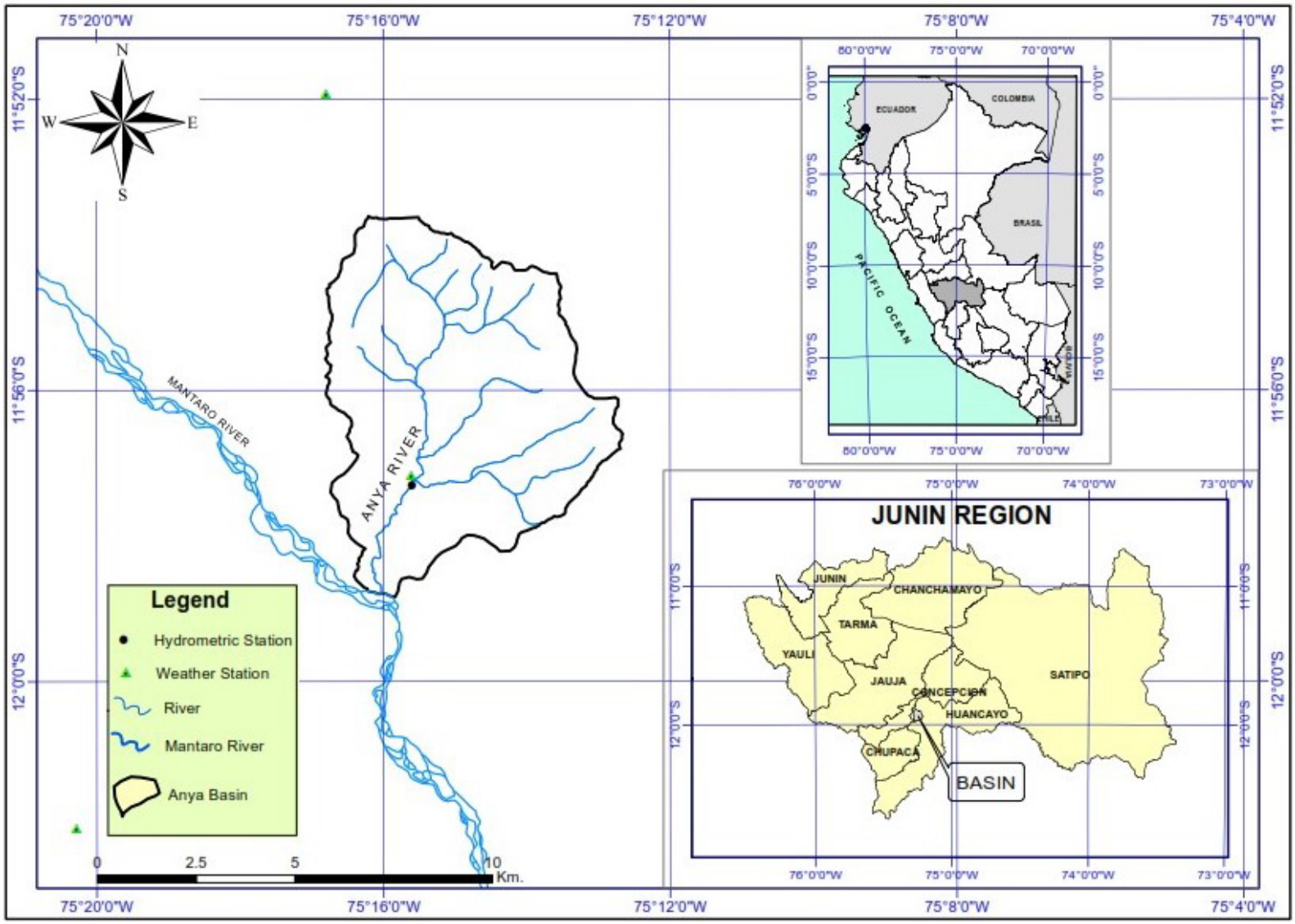

Figure 1. Location of the Anya basin, Junin, Peru.

The plant cover updated to October 2019 is composed of 41.4 % of crops, the most representative of the area being: potatoes, corn, barley, broad beans, olluco and oats, mainly for self-consumption; 18.9 % eucalyptus forest plantations; 26.1 % grasslands; 8.5 % Andean scrublands typical of sub-humid mountains, and the remaining 5.1 % corresponds to the urban area. The dominant soils are 70% loam and 30 % clay loam, with a pH between 3.8 to 6.6, predominantly acid. According to PDC (2013), in terms of socioeconomic characteristics of the basin, the observed trend is towards the intensification of the urbanization process, which is manifested in 67 % of the urban population and 33 % of the rural population (Guabloche & Saldarriaga, 2013).

Data source and processing

Climatic data

For the Anya basin, there are no daily climatic data of sufficient length, which, according to the OMM (2017), must be 30 years for the calculation of the standard climatological normals, so the daily precipitation and temperature data set in grid was used. PISCO from SENAMHI (National Service of Meteorology and Hydrology of Peru) in the period from January 1981 to December 2015. PISCO is based on pluviometric data from Peru and CHIRPS satellite information (Funk, Peterson, & Landsfeld, 2015) in a 0.05° × 0.05° spatial resolution grid. The greater precision of

precipitation estimates with PISCO is limited to calibrated regions, such as the Pacific coast and the eastern and western slopes of the Andes of Peru (Aybar *et al*., 2017; Llauca, Lavado-Casimiro, Montesinos, Santini, & Rau, 2021). In addition, PISCO is used by SENAMHI in Peru for operational purposes, for the monitoring of droughts and floods on a national scale, and was applied, for example, for the hydrological modeling of the Andean Vilcanota river basin (Fernandez-Palomino, Hattermann, Krysanova, Vega-Jácome, & Bronstert, 2021) and other Peruvian basins (Llauca *et al*., 2021). The use of PISCO is relatively recent in hydrological studies and must be accompanied by the use of commands in R language to extract information in previously indicated coordinates (Asurza & Lavado, 2020). The PISCO dataset is publicly available at https://piscoprec.github.io/ and is intended to support hydrological studies and water management practices (Aybar *et al.*, 2020).

In this case, the coordinates of three stations, one within the basin, were used for the PISCO validation, using the correlation coefficient between the precipitation data measured between December 2013 and March 2015 and gridded PISCO precipitation of the same period (Table 1). It was not necessary to carry out the process of correcting the bias of the data obtained with PISCO, due to the size of the basin (< 100 km^2), since a single pixel covers the entire basin, that is, the precipitation data of a pixel represent the average rainfall of the basin of interest and is sufficient for hydrological modeling. The mean discharge data (m^3/s) used for the calibration and validation of the model were recorded at the Anya hydrometric station, by the VLIR-UNALM program (VLIR & UNALM, 2015).

Solar radiation (MJ/m^2s^2), wind speed (m/s), and relative humidity (%) data were generated by the SWAT weather simulation tool.

Table 1. Scale reduction points of Peruvian Interpolated data of the SENAMHI´s Climatological and hydrological Observations (PISCO).

Point	Station	Latitude (°)	Length (°)	Altitude (masl)
X_1	Anya	-11.9552	-75.2600	3 279
X_2	Ingenio	-11.8653	-75.2800	3 390
X_3	Huayao	-12.0335	-75.3381	3 360

Soil data, vegetation cover and topography

We worked with the updated Vegetal Cover map as of October 2019, defined and digitized from PlanetScope images from the SkySat-C satellite (launched in 2016), spatial resolution of 3 meters, 4 bands (RGB, NIR) and digital format. GeoTIFF file. The soil map was obtained from the Ecological and Economic Zoning of the Junín region (MINAM, 2015) projected in the Universal Transversal Mercator (UTM) coordinate system, Datum and reference ellipsoid WGS-84, scale 1/100,000, available from the geo server of the Ministry of the Environment of Peru -MINAM- https://geoservidor.minam.gob.pe/. The Digital Elevation Model of the ASTER satellite (MED) Version 3 was used, with spatial resolution of 1 arc second (approximately 30 meters of horizontal position in the terrestrial equator). Within ArcMap 10.5 the ArcSWAT extension downloaded from

https://swat.tamu.edu/ compatible with the version of ArcMap was loaded.

Data from Global Climate Models (GCMs)

For comparative purposes between RCP 4.5 and RCP 8.5 scenarios, monthly precipitation and temperature data from five models belonging to CMIP5 (Coupled Model Intercomparison Project Phase) obtained from the Climate Explorer climate explorer page were used: https://climexp.knmi.nl/start.cgi (European climate data and evaluation set), choosing models that best represent the synoptic systems that modulate the climate of South America (Acuña, Flores, Llacza, & Rorher, 2019). Global models are capable of reproducing the basic characteristics of the current seasonal cycle of precipitation, however, there are some discrepancies in quantitatively reproducing the seasonal accuracy over the main basins of the continent (Lujano, Hidalgo, Diaz, Tapia, & Lujano, 2016), and therefore, its evaluation is desirable. RCPs 4.5 and 8.5 were selected because they represent a stable extreme and high-level climate change projection (Ashu & Lee, 2020). The RCP 4.5 scenario suggests a world using technologies and strategies that lead to a stabilized radiative forcing of 4.5 W/m^2 in 2100. In contrast, the RCP 8.5 scenario warns that high population growth, lack of developed technologies and the high emissions of Greenhouse Gases (GHGs) favor radiative forcing reaching 8.5 W/m^2 in 2100, being the most critical of the CMIP5 (González-Celada *et al*., 2021).

To find the variation of the future climate, the delta change methodology was applied (Ramírez & Jarvis, 2010), with which the variations between the simulations of the current and future climate models could be estimated, adding the changes to the observed time series. The absolute sum was used for temperatures (in degrees centigrade) and the relative changes for precipitation (in percentage), taking the base period from 1980 to 2010 and the future period from 2070 to 2100 (Table 2), for each model of the Table 3.

Table 2. Delta change of precipitation and monthly temperatures.

$\mathbf{PREC.camb} = \left(\frac{\mathbf{PREC.fut} - \mathbf{PREC.hist}}{\mathbf{PREC.hist}}\right)\mathbf{x100\%}$	$\mathbf{T.camb} = \mathbf{T.fut} - \mathbf{T.hist}$
• PREC.change = Precipitation change (%)	• T.change = Temperature change (ºC)
• PREC.fut. = Multiannual average of accumulated precipitation (2070-2100), annual average (time series)	• T.fut. = Multiannual average temperature (2070-2100) annual average (time series)
• PREC.hist.= Multiannual average of seasonal or annual accumulated precipitation (1980-2010)	• T.hist.= Multiannual average of the seasonal or annual accumulated temperature (1980-2010)

Table 3. Global Climate Models (GCMs) analyzed in this study.

Nº	Model name	Country	Atmospheric resolution (km)
1	ACCES1.0	Australia	192 x 145
2	bcc-csm1-1	China	281 x 279
3	BNU-ESM	China	142
4	GISS-E2-rp2	USA	110 x 110
5	CMCC-CM	Italy	82.5 x 82.5

The multiplicative correction factor was used to correct the precipitation overestimates of the GCMs according to the following equation:

$$Fc = \frac{Pobs}{Psim} \quad (1)$$

Where *Fc* is the correction factor, *Pobs* is the observed precipitation and *Psim* is the simulated precipitation of a given model. Then the modified rainfall and temperatures according to the variations established in the delta change, were used as input to simulate the future flows in the SWAT.

Table 4 contains the description and source of the watershed data used for hydrological modeling with SWAT.

Table 4. Anya basin description and data source used in SWAT.

Data	Font	Spatial/temporal resolution
Digital Elevation Model (DEM)	ASTER version 3. https://lpdaac.usgs.gov/products/astgtmv003/	12.5 m
Coverage and land use map	SkySat-C satellite. PlanetScope images	3 m
Soil map	Ecological Economic Zoning Junín https://geoservidor.minam.gob.pe/	3 m
Daily precipitation data (mm), maximum temperature (°C) and minimum temperature (°C)	PISCO: http://www.senamhi.gob.pe/?p=observacion-de-inundaciones (Period 1981-2015)	5 km/day
Observed precipitation (mm)	Seasons Anya, Ingenio y Huayao (2013-2015)	
Downloads (m^3/s)	Hydrometric station Anya. Program VLIR-UNALM (2013-2015)	Average/day
Global Climate Models	Climate Explorer: https://climexp.knmi.nl/start.cgi	Average 150 km

Tecnología y Ciencias del Agua

OPEN ACCESS

Check for updates

SWAT model calibration and validation

Given the small length of the flow record, the simulation period was from August 2012 to March 2015, with the model's heating period defined as 16 months (August 2012 – November 2013). 10 months were used for calibration and the rest for validation (06 months), that is: calibration (December 2013 – September 2014) and validation (October 2014 – March 2015). The manual parameter calibration option of the SWAT program was used, considering the efficiency measures proposed by Moriasi *et al*. (2007), including Nash-Sutcliffe efficiency (NSE), bias percentage (PBIAS) and coefficient of determination (R^2). R^2 indicates the strength of the linear relationship between the observed and simulated values, ranging from 0 to 1, where 1 indicates a perfect match. NSE is a normalized statistic that establishes the relative magnitude of the residual variance ("noise") compared to the variance of the measured data ("information") (Nash & Sutcliffe, 1970). NSE shows how well the plot of observed versus simulated data fits the 1:1 line varying between -∞ and 1, with NSE = 1 being the optimal value. The performance of the model is considered satisfactory when R^2 and NSE are greater than 0.5 for discharge (Moriasi *et al*., 2007). The percentage bias (PBIAS), which underestimates the average tendency of the calibrated data to be larger or smaller than the observed data, is used as an indicator of model performance (Gupta, Sorooshian, & Yapo, 1999). The optimal value is zero, and low absolute values indicate better simulations. In monthly time steps, a PBIAS of less than 25 % for stream flow after calibration is considered satisfactory (Moriasi *et al*., 2007). General information about

the evaluation criteria and/or model performance ratings is shown in Table 5.

Table 5. Performance ratings by statistical methods. NSE: Nash-Sutcliffe efficiency; PBIAS: percentage bias; R^2: coefficient of determination.

NSE	PBIAS	R^2	Performance rating
0.75 < NSE ≤ 1.00	PBIAS ≤ ± 10	0.75 < R^2 ≤ 1.00	Very good
0.60 < NSE ≤ 0.75	± 10 < PBIAS ≤ ± 15	0.60 < R^2 ≤ 0.75	Okay
0.36 < NSE ≤ 0.60	± 15 < PBIAS ≤ ± 25	0.50 < R^2 ≤ 0.60	Satisfying
0.00 < NSE ≤ 0.36	± 25 < PBIAS ≤ ± 50	0.25 < R^2 ≤ 0.50	Bad
NSE ≤ 0.00	± 50 ≤ PBIAS	0.50 ≤ R^2	Inappropriate

Source: Adapted from Moriasi *et al.* (2007).

Results

Monthly precipitation and temperature in PISCO grid

The statistics of the multiannual precipitation and temperature series for the Anya basin, obtained with PISCO between 1981 and 2015, were calculated. The total multiannual precipitation was 741.8 mm, with the months of greatest and least precipitation being February and July, respectively; the resulting multiannual average temperature was 11.2°C,

with higher temperatures in December and January, with July being the coldest month (Table 6). The month with the highest rainfall was February, with the dry months being the ones with the lowest standard deviation (Figure 2).

Table 6. Precipitation and temperature statistics in the Anya basin between 1981 and 2015.

Month	Precipitation (mm)				Temperature (°C)			
	Avg.	**Min.**	**Max.**	**S.D.**	**Avg.**	**Min**	**Max**	**S.D.**
Jan	122.5	63.8	206.6	34.4	12.4	11.3	13.8	0.58
Feb	132.8	50.2	233.7	40.6	12.1	11.2	13.8	0.63
Sea	117.9	63.5	169.4	30.9	11.8	10.9	13.2	0.59
Apr	54.5	24.2	115.5	21.4	11.2	10.3	12.7	0.52
May	14.8	1.5	32.0	7.4	10.4	9.0	11.3	0.55
Jun	5.6	0.0	35.3	6.4	9.8	8.9	10.9	0.56
Jul	4.0	0.0	21.4	4.1	9.1	7.9	10.3	0.55
Aug	11.4	0.1	31.6	8.6	10.2	9.5	11.4	0.49
Sep	33.0	10.8	70.6	13.0	11.2	10.2	12.3	0.47
Oct	63.8	19.8	124.8	21.4	12.0	11.2	12.7	0.37
Nov	71.0	31.5	143.4	25.5	12.3	11.6	13.0	0.40
Dec	110.4	48.1	179.3	30.7	12.4	11.6	13.3	0.36
Min.	**4.0**	**0.0**	**21.4**	**4.1**	**9.1**	**7.9**	**10.3**	**0.4**
Max.	**132.8**	**63.8**	**233.7**	**40.6**	**12.4**	**11.6**	**13.8**	**0.6**

Note: Total precipitation 741.8 mm and average annual temperature 11.2°C.

Source: Prepared with the PISCO database.

Tecnología y Ciencias del Agua

OPEN ACCESS

Check for updates

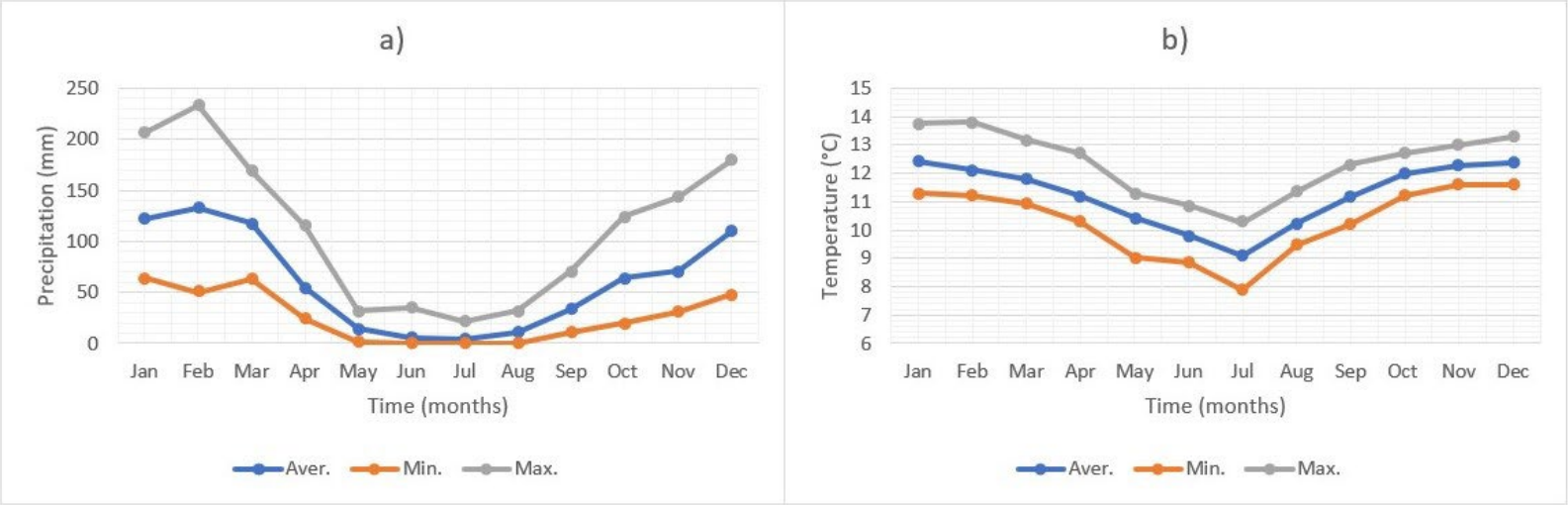

Figure 2. Precipitation (a) and temperature (b) in the Anya basin obtained from the PISCO database (1981 – 2015).

Figure 3 shows the trend behavior of both variables in the period between 1981 and 2015, noting that precipitation had a slight increase, however, temperature had a significant increase of approximately 0.8 °C in the period considered, verifying the trend of area heating. It is important to highlight that, in the last two decades of the 20th century, Peru faced two strong intensity coastal El Niño Phenomena: the first, in the period 1982-1983 and the second, in the period 1997-1998 (SENAMHI, 2014), which is why Figure 3b shows a notable increase in temperature in the years 1983 and 1998, demonstrating the influence of the coastal El Niño Phenomenon on the temperatures of the Anya inter-Andean basin. Regarding precipitation, the results are not conclusive, but

it is noted that in the 1983 event precipitation decreased, because warming in the Central Pacific can suppress rain in the upper parts of the basins (Lavado & Espinoza, 2014). However, in 1998 the total annual precipitation was equal to the average for the area.

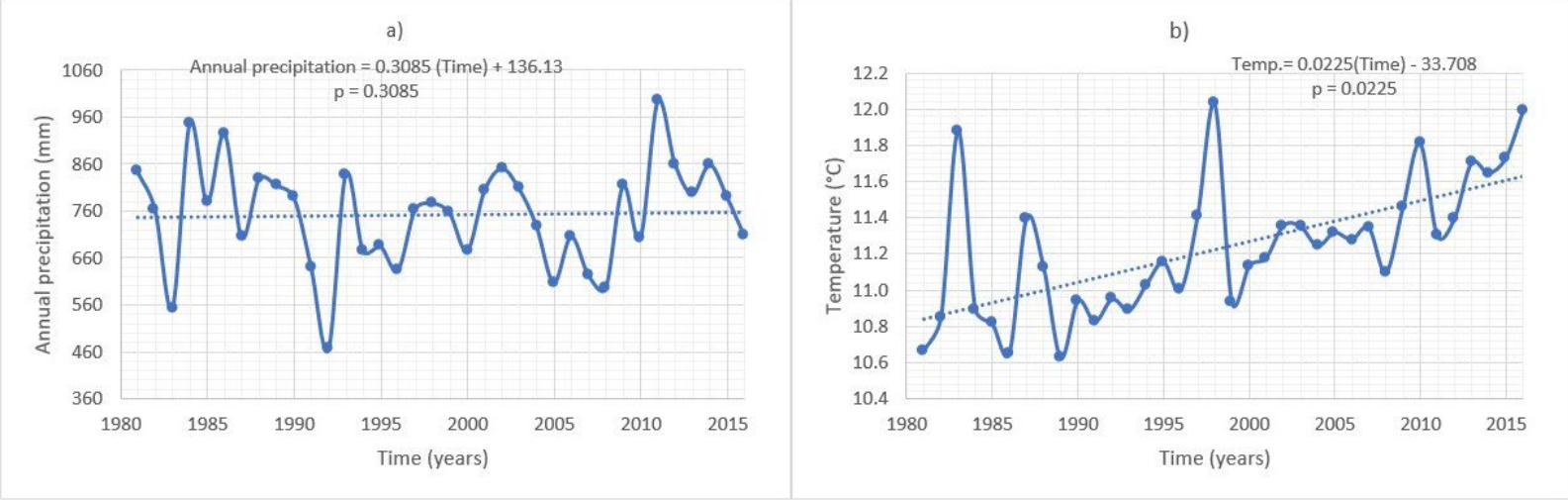

Figure 3. Precipitation (a) and temperature (b) trends in the Anya basin obtained from the PISCO database (1981-2015).

PISCO gridded data application

In principle, the level of correlation between the registered monthly average precipitation data (data obtained for the basin between 2013 and 2015) and the average precipitation obtained from the PISCO database for the same period was established, obtaining a determination coefficient R^2 = 0.91 (very good) (Figure 4). In the same way, for the average

monthly temperature, a determination coefficient R^2 = 0.63 (good) was obtained, which allowed us to verify that the data obtained with the grilled product PISCO are adequate to be entered into the SWAT model in longer periods.

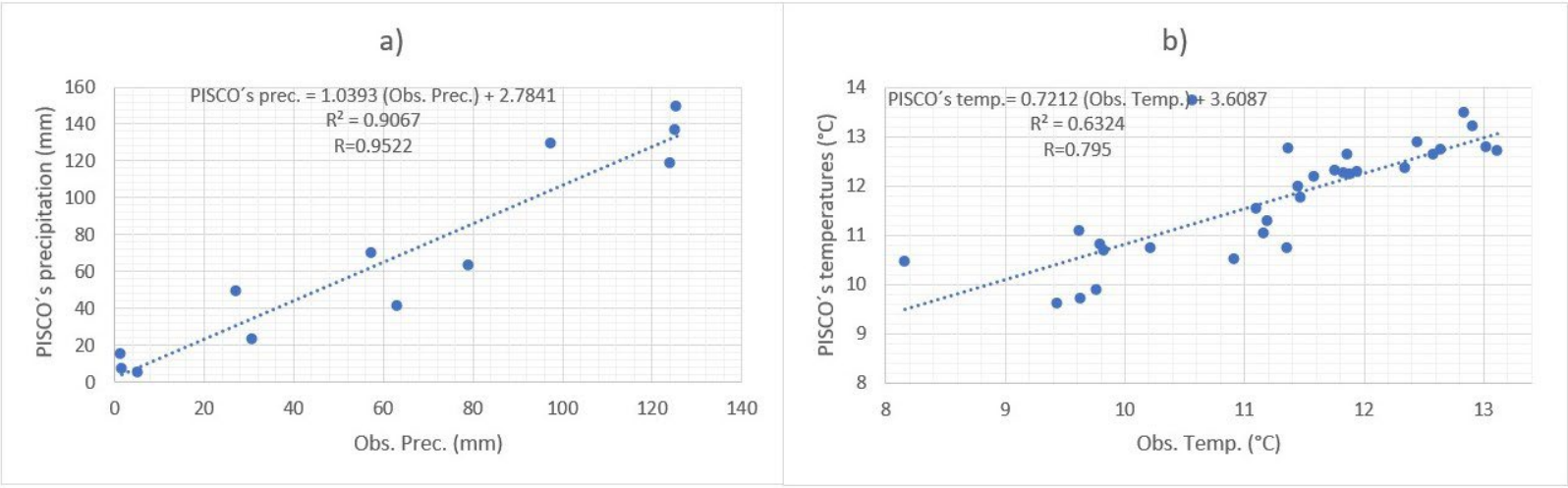

Figure 4. Correlation between observed monthly data (2013-2015) and PISCO gridded data: a) precipitation, b) temperature.

Validation of CMIP5 models-precipitation and temperature projected with GCMs

When comparing the rainfall obtained with the PISCO database and those simulated with the GCMs in the basin for the period 1981-2015, an overestimation of the simulated rainfall with respect to those obtained with PISCO is noted (Figure 5a), as reported Lujano *et al.* (2016) for the

Peruvian highlands. However, despite the fact that they do not accurately quantify the observed values, it is evident that the outputs of the GCMs adequately reproduce the seasonality of precipitation in the area, for which the coefficient of determination (R^2) between observed and simulated precipitation is "very good" in all cases (Table 7). Regarding temperature, all the GCMs also overestimate it, verifying that the thermal range is not being adequately represented, and noting ranges lower than the observed 3.3 °C.

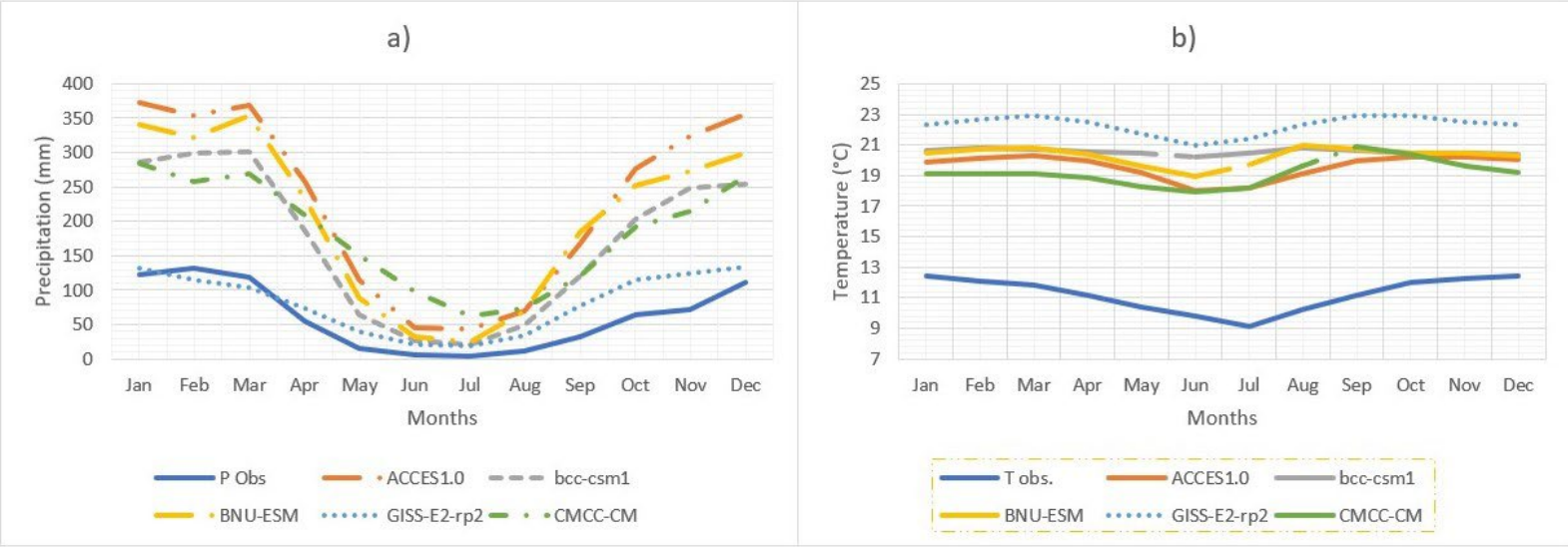

Figure 5. Precipitation (a) and Temperature (b) according to GCMs versus PISCO database in the period 1981-2015.

Table 7. Determination coefficients (R^2) of the precipitation variable calculated from the PISCO database and data simulated with GCMs in the period 1981-2015.

GCM	R^2
ACCES1.0	0.915
bcc-csm1	0.941
BNU-ESM	0.907
GISS-E2-rp2	0.791
CMCC-CM	0.900

The average monthly precipitation values of the GCMs were reduced by the multiplicative factor estimated using Equation (1). Next, the variation of monthly precipitation and temperature was calculated through the difference between the results of the models in the future period (2070 -2100) and the base period (1980-2010) (delta change). The evaluation of climate change to 2100 in the RPC 4.5 scenario and the five GCMs, gives as a result that, in four models, an increase in precipitation in the basin is expected and only in one case -BNU-ESM model- the total precipitation annual would decrease (-0.51 %); however, in the average of the models, the variation of the percentage of precipitation will be 4.63 %. In general, future precipitation is very complex and uncertain because there are differences between RCP and MCGs scenarios. Regarding the temperature in the RCP 4.5 scenario, the annual average increase will be 2.3 °C. In the RCP 8.5 scenario, an

increase in the annual average percentage of precipitation of 8.14 % and temperature of 4.5 °C is expected (Figure 6). The results are similar to those reported by SENAMHI researchers, who indicate that there will be a progressive increase in maximum and minimum temperatures throughout the area in relation to the current climate (Avalos *et al*., 2013).

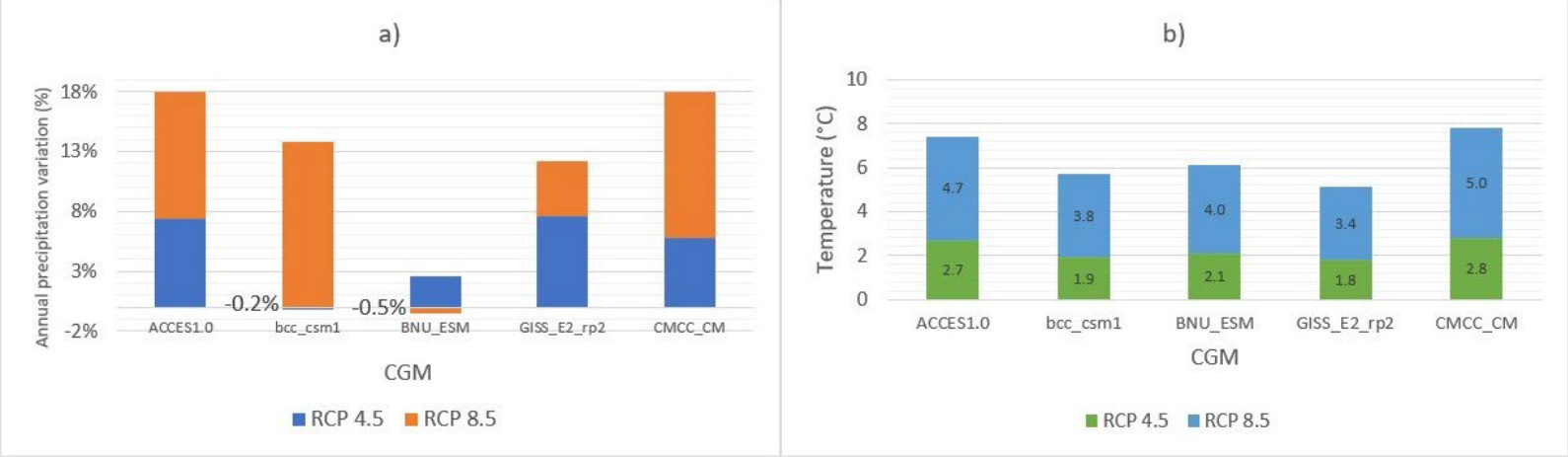

Figure 6. Precipitation (a) and Temperature (b) projections with the five GCMs to 2100 in RCP 4.5 and 8.5 scenarios.

Selected parameters of the SWAT model

For the calibration of the model, a total of 12 potentially influential parameters were defined and selected manually, having as reference, the parameters selected for the Andean basin of the Vilcanota River by

Fernandez-Palomino *et al*. (2021), related to the base flow, the unit of hydrological response and roughness (Arnold, Moriasi, & Gassman, 2012). The parameter CN2 (Curve Number in humidity condition II, intermediate), related to surface runoff, was varied. Among the calibrated SWAT parameters, only two (SOL_AWC, GW_REVAP) can alter the water balance since they influence evapotranspiration and, subsequently, the estimation of runoff. The remaining parameters influence groundwater (GW_DELAY, RCHRG_DP, GWQMN, ALPHA_BF) and flow routing (CH_N2) without affecting system water loss. The RCHRG_DP parameter indicates the volume of water filtered in the deep aquifer in relation to the total recharge that enters the aquifers and provides an idea of the recharge that enters the deep aquifers in the Peruvian Andean basins, which sustain the prolonged flow of the dry season in these basins (Fernandez-Palomino *et al*., 2021). The selected parameters and calibrated results are shown in Table 8.

Tecnología y Ciencias del Agua
OPEN ACCESS
Check for updates

Table 8. SWAT model parameters used in the Anya basin.

Item	Parameter	Definition	Value	Best simulation
			initial	Simulation 21
1	*R_CN2.mgt	SCS Curve Number for humidity condition II.	*	+4 %
2	V_ALPHABF.gw	Baseflow alpha factor (d).	0.048	0.4
3	V_GWDELAY.gw	Groundwater offset (d).	31	60
4	V_GWQMN.gw	Water table threshold level to initiate return flow (mm).	1 000	1 000
5	V_GWREVAP.gw	Groundwater revaluation coefficient.	0.02	0.182
6	V_RCHRGDP.gw	Percolation fraction of the deep aquifer.	0.05	0.05
7	V_REVAPMN.gw	Depth of the surface aquifer to produce evaporation (mm).	750	1050
8	V_CANMX.hru	Maximum storage of the vegetal cover.	0	15
9	V_ESCO.hru	Soil ET Compensation Factor.	0.95	0.64
10	V_EPCO.hru	Compensation factor for plant uptake.	1	0.7
11	R_CHN2.rte	Main channel Manning´s coefficient.	0.014	0.137
12	*R_SOLK.sol	Saturated hydraulic conductivity (mm h^{-1})	*	-4 %

*Varies according to soil type.

Tecnología y Ciencias del Agua
OPEN ACCESS
Check for updates

SWAT model calibration and validation

The PBIAS value for the flow calibration and validation in the Anya River is positive, indicating the underestimation of the model. The difference between the simulated and observed values can be attributed to several factors, basically the little data on registered flows does not allow automatic calibration and validation, which is necessary to use the SWAT CUP. The sources of uncertainty in this case are measurement errors, instrument errors, and model errors. However, based on the values of NSE and R^2, the calibration and validation results are satisfactory (Table 9).

Table 9. Statistical indicators of monthly performance of the model.

Indicator	Calibration stage	Performance rating	Validation stage	Performance rating
NSE	0.62	Good	0.46	Satisfying
PBIAS	6.72 %	Very good	7.43 %	Very good
R^2	0.81	Very good	0.96	Very good

Tecnología y Ciencias del Agua

OPEN ACCESS

Check for updates

Assessment of climate change in future discharges (2070-2100)

After calibration, the adjusted precipitation and temperature were incorporated into the SWAT hydrological model according to the variations by RCP scenario and by MCG, keeping the topography, basin division and soil type constant. Table 10 contains the simulated monthly discharges in current condition, and the simulated discharge outputs in SWAT with modified climatic data according to the five GCMs tested. The annual average of the GCMs showed an increase of +2.4 % and +12.6 % in the RCP 4.5 and 8.5 scenarios, respectively. Figure 7 shows the monthly average discharge hydrographs projected in the Anya basin for the period 2070 - 2100 in the RCP 4.5 and RCP 8.5 emission scenarios, respectively. An increase in runoff is visualized in the humid months, reaching its highest level of variation in March. It is evident that the average downloads would increase in the months of April and May, a result similar to that obtained by Lujano *et al*. (2016) in the Ramis river basin in Puno, however, the discharges would decrease in the months of July to December.

Tecnología y Ciencias del Agua

OPEN ACCESS

Check for updates

Table 10. Simulated average monthly discharges current and in the horizon 2070 - 2100 in m^3/s.

Month	Current sim flow	Acces 1.0 4.5	Acces 1.0 8.5	bcc - csm 4.5	bcc - csm 8.5	BNU - ESM 4.5	BNU - ESM 8.5	CMCC - CM 4.5	CMCC - CM 8.5	GISS - E2 4.5	GISS - E2 8.5
Jan	1.01	0.96	1.01	0.82	1.20	1.02	1.00	0.91	1.22	0.68	0.81
Feb	1.11	1.22	1.29	1.05	1.32	1.27	1.23	1.30	1.46	0.89	1.07
Mar	1.40	1.52	1.63	1.49	1.63	1.45	1.46	1.64	1.93	1.44	1.41
Apr	0.91	1.21	1.27	1.15	1.28	1.18	1.19	1.28	1.43	1.21	1.14
May	0.56	0.89	0.93	0.84	0.93	0.82	0.82	1.00	1.14	0.83	0.79
Jun	0.16	0.14	0.15	0.12	0.15	0.11	0.10	0.18	0.24	0.04	0.11
Jul	0.04	0.04	0.04	0.04	0.05	0.04	0.04	0.05	0.06	0.03	0.04
Aug	0.03	0.03	0.03	0.03	0.03	0.03	0.03	0.03	0.04	0.02	0.03
Sep	0.06	0.06	0.07	0.06	0.07	0.07	0.05	0.05	0.06	0.07	0.06
Oct	0.04	0.03	0.03	0.03	0.04	0.03	0.03	0.03	0.04	0.04	0.03
Nov	0.22	0.09	0.09	0.07	0.11	0.09	0.06	0.09	0.11	0.06	0.08
Dec	0.97	0.79	0.81	0.62	0.84	0.83	0.68	0.84	1.01	0.35	0.63
Half	0.54	0.58	0.61	0.52	0.64	0.58	0.56	0.62	0.73	0.47	0.52
Max.	1.40	1.52	1.63	1.49	1.63	1.45	1.46	1.64	1.93	1.44	1.41
Min.	0.03	0.03	0.03	0.03	0.03	0.03	0.03	0.03	0.04	0.02	0.03
Var.		7.4 %	13.1 %	-3.0 %	17.4 %	6.6 %	3.1 %	14.0 %	34.4%	-12.8 %	-4.7 %

Tecnología y Ciencias del Agua

OPEN ACCESS

Check for updates

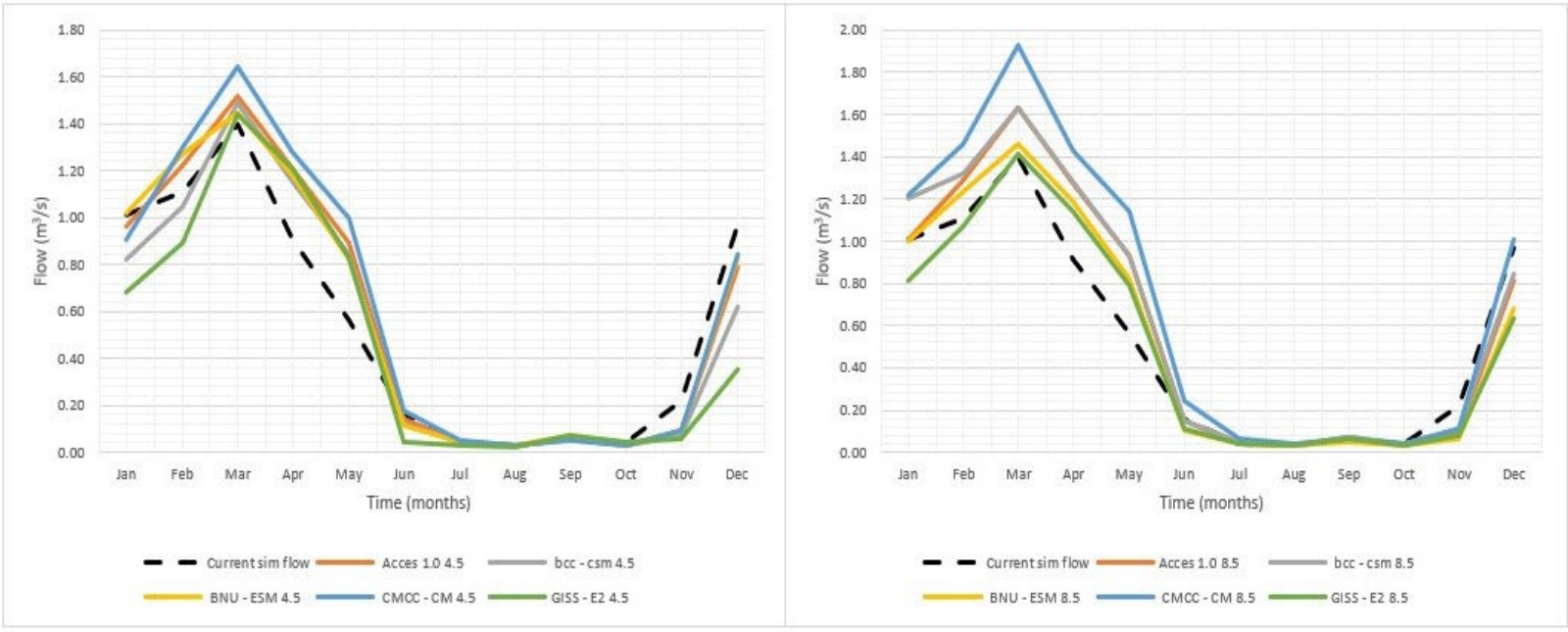

Figure 7. Variation of discharges from the Anya River in climate scenarios RCP 4.5 and 8.5 in the 2070-2100 horizon.

Discussion

With the PISCO gridded product, limitations are being overcome in the use of mathematical models in many basins of Peru, due to the scarcity of daily precipitation data, since it allows a greater number of basins to be calibrated for operational purposes of daily flow forecasting, using different hydrological models (Aybar *et al*., 2017). Satellite-based precipitation products are promising alternative sources for regions with few observations. However, it is necessary to use terrestrial data to reduce the bias of these estimates, since they can be erroneous or biased

(Fernandez-Palomino *et al*., 2022). However, the highest precision of precipitation estimates with PISCO is obtained in calibrated regions such as the Pacific coast and the eastern and western slopes of the Andes of Peru (Aybar *et al*., 2020, Llauca *et al*., 2021). Therefore, it is confirmed that PISCO is valid in regions of the Peruvian highlands, with high correlation coefficients (Salas, 2019), so its use for the Mantaro valley in Junín is efficient and reliable. The results show that the SWAT model correctly represents the seasonality of the main components of the hydrological cycle. However, the model does not correctly quantify the high flow rates during wet periods, as reported by Asurza and Lavado (2020), concluding that it can be used as support for studies of water balance and water management in the Peruvian Pacific drainage. The approach and methods developed can be replicated in any other region of Peru.

For the calibration of the model, in the Anya basin there are limitations of observed data, a typical characteristic of poorly instrumented basins; however, Arnold, Srinivasan, Muttiah and Williams (1998) mention that SWAT does not require calibration to fulfill its prediction purpose in this type of basin. However, a good calibration fit of the monthly mean flow was achieved, which allowed the use of the SWAT model for the projection of climate change in the future discharges of the basin. Sometimes uncertainties due to the quality of the observed data prevent good hydrological modeling. Therefore, further studies are needed to quantify uncertainties in hydrological modeling due to errors in discharge data observed in Andean basins (Fernandez-Palomino, 2021).

The precipitation anomaly plays an important role in the probability of flooding and erosion in the basin, since the amount and intensity of rainfall are the main factors that change with climate change (González-Celada *et al*., 2021). and it is what can be verified in the behavior of precipitation in the area today, noting that in the Anya basin, temperatures are higher and precipitation is more intense and of short duration. These results indicate the increase in the concentration of rainfall events throughout the 21st century, suggesting that individual rainfall events may have greater physical potential for erosion risk by the end of the century (Wongchuig *et al*., 2018). From the climatic point of view, it is known that a monthly average of precipitation provides valuable information on the pluviometry of a territory, but it does not say anything about the frequency or number of rainy days, nor about the breakdown of the quantities registered in the rainy days (Sarricolea & Romero, 2015). Water erosion in the Anya basin is greater in the months of high rainfall, due to the geomorphological and landscape characteristics of the study area, where the topographic factor is an indicator of steep slopes and, therefore, of greater intensity of erosive processes (Del Águila & Mejía, 2021).

Analyzing climate change in regions located in the central Andes, Acuña *et al*. (2019) obtained similar results in terms of precipitation using three CMIP3 global models, with a possible annual precipitation variation of ± 15 % in the worst emissions scenario, which will have a direct impact on discharges. Likewise, Álvarez and Villaverde (2015), carrying out hydrological modeling in the face of climate change in the Lurín river basin (Pacific Ocean slope - Peruvian coast), determined that there will be an

increase in the availability of water resources (increase in flows) and the wet and dry periods will be more intense in the future. Pilares (2018) in his research for the Cabanillas river basin in Puno (slope of Lake Titicaca - southern high Andean zone of Peru), found that the average annual variation of discharges is positive in all the scenarios and models tested.

Conclusions

Currently, in the Anya basin, climate change is manifested in the alteration of the temperature and precipitation variables. The average results show an increase in precipitation between 4.63 and 8.14 %, and temperature between 2.3 and 4.2 °C, in RCP 4.5 and 8.5 scenarios by 2100, respectively. For the evaluation of future climate change, information was extracted from five global climate models (GCMs) in two emission scenarios (RCP 4.5 and 8.5) to simulate them in SWAT. It was possible to verify that, for both scenarios, there will be an increase in precipitation and temperature in the area, which will affect the increase in surface runoff. Therefore, it is concluded that in the Anya basin, there will be an increase in flows in both emission scenarios; 2.4 % in RCP 4.5 and 12.6 % in RCP 8.5. However, it should be noted that climate change projections contain several uncertainties associated with the resolution of global climate models, however, these results show the potential vulnerability of agriculture in global warming conditions.

The statistical indicators of the goodness of fit of hydrological models show that the SWAT model allows reproducing the runoff capacity

of the Anya basin, whose execution was carried out in a GIS environment, using the input maps of coverage and soil types, which they can be updated from satellite images, as in this case, in which the vegetation cover map was updated. In addition, the SWAT model proved to be very useful for modeling climate change from records obtained from databases such as PISCO from SENAMHI and global climate models (GCMs).

Regarding the probable increase in flows influenced by climate change, it is important to carry out adequate management of the water resource in the Anya basin, respecting the marginal strips of the river and avoiding all types of construction in them. Likewise, soil conservation practices (gully control) and reforestation should be continued, preferably with native species. The importance of hydrological monitoring and knowledge of the dynamics of use and management of water resources is highlighted, to achieve better hydrological adjustments in areas of high anthropic intervention, increasing the potential use of hydrological modeling as a planning tool.

Acknowledgment

The authors express our gratitude to the National University of San Cristóbal de Huamanga and the National University of the Center of Peru, institutions where we are allowed to practice teaching and research.

References

Abbaspour, K. C., Vaghefi, S. A., & Srinivasan, R. (2017). A guideline for successful calibration and uncertainty analysis for soil and water assessment: A review of papers from the 2016 international SWAT conference. *Water* (Switzerland), 10(1). Recovered from https://doi.org/10.3390/w10010006

Acuña, D., Flores, W., Llacza, A., & Rorher, M. (2019). Escenarios futuros de cambio climático desde modelos globales para localidades de los Andes centrales. *Anales Científicos*, 80(2), 476-494. Recovered from https://dialnet.unirioja.es/servlet/articulo?codigo=7546798

Almeida, R. A., Pereira, S. B., & Pinto, D. B. (2018). Calibration and validation of the SWAT hydrological model for the Mucuri river basin. *Engenharia Agrícola*, 38(1), 55-63. Recovered from https://doi.org/10.1590/1809-4430-Eng.Agric.v38n1p55-63/2018

Álvarez, T., & Villaverde, R. (2015). *Balance hídrico futuro en la cuenca del rio Lurín a través de la modelación hidrológica ante el cambio climático* (tesis de grado). Universidad Nacional Agraria La Molina. Lima, Perú. Recovered from http://repositorio.lamolina.edu.pe/handle/UNALM/2157

Arnold, J. G., Srinivasan, R., Muttiah, R. S., & Williams, J. R. (1998). Large area hydrologic modeling and assessment part I: Model development. *Journal of the American Water Resources Association*, 34(1), 73-89. Recovered from https://doi.org/10.1111/j.1752-1688.1998.tb05961.x

Arnold, J. G., Moriasi, D. N., & Gassman, P. W. (2012). SWAT: Model use, calibration, and validation. *American Society of Agricultural and Biological Engineers*, 55(4), 1491-1508. Recovered from https://swat.tamu.edu/media/99051/azdezasp.pdf

Ashu, A., & Lee, S. (2020). Reutilización de agua de drenaje agrícola en una cuenca de uso de suelo mixto. *Agronomía*, 9(1), 6. Recovered from https://doi.org/10.3390/agronomy9010006

Asurza, F., & Lavado, W. (2020). Estimación de parámetros regionales del modelo SWAT: metodología y aplicación a cuencas hidrográficas en el drenaje del Pacífico peruano. *Agua*, 12(11), 3198. Recovered from https://doi.org/10.3390/w12113198

Aybar, C., Lavado-Casimiro, W., Huerta, A., Fernández, C., Vega, F., Sabino, E., & Obando, O. (2017). *Uso del producto grillado "PISCO" de precipitación en estudios, investigaciones y sistemas operacionales de monitoreo y pronóstico hidrometeorológico* (Nota Técnica 001 SENAMHI–DHI-2017). Lima-Perú. Recovered from https://www.senamhi.gob.pe/load/file/01402SENA-8.pdf

Aybar, C., Fernández, C., Huerta, A., Lavado, W., Vega, F., & Felipe-Obando, O. (2020). Construction of a high-resolution gridded rainfall dataset for Peru from 1981 to the present day. *Hydrological Science Journal,* 65(5), 770-785. Recovered from https://doi.org/10.1080/02626667.2019.1649411

Avalos, G., Oria, C., Jacome, G., Acuña, D., Llacza, A., & Cubas, F. (2013). *Cambio climático en la cuenca del río Mantaro. Proyecciones para el año 2030*. Lima, Perú: Servicio Nacional de Meteorología e Hidrología.

Del Águila, S., & Mejía, A. (2021). Caracterización morfométrica de dos cuencas altoandinas del Perú utilizando sistemas de información geográfica. *Tecnología y ciencias del agua*, 12(2), 538-562. Recovered from https://doi.org/10.24850/j-tyca-2021-02-12

Deng, C., Pisani, B., Hernández, H., & Li, Y. (2020). Assessing the impact of climate change on water resources in a semi-arid in central Mexico using a SWAT model. *Boletín de la Sociedad Geológica Mexicana*, 72(2), 1-19. Recovered from http://dx.doi.org/10.18268/BSGM2020v72n2a150819

Fernandez-Palomino, C. A., Hattermann, F. F., Krysanova, V., Vega-Jácome, F., & Bronstert, A. (2021). Towards a more consistent eco-hydrological modelling through multi-objective calibration: A case study in the Andean Vilcanota River basin, Peru. *Hydrological Science Journal*, 66, 59-74. Recovered from https://doi.org/10.1080/02626667.2020.1846740

Fernandez-Palomino, C. A., Hattermann, F. F., Krysanova, V., Vega-Jácome, F., Lavado, W., Santini, W., Aybar, C., & Bronstert, A. (2022). A novel high-resolution gridded precipitation dataset for Peruvian and Ecuadorian watersheds: Development and hydrological evaluation. *Journal of Hydrometeorology*, 23(3), 309-336. Recovered from https://doi.org/10.1175/JHM-D-20-0285.1

Funk, C., Peterson, P., & Landsfeld, M. (2015). The climate hazards infrared precipitation with stations-a new environmental record for monitoring extremes. *Scientific Data*, 2, 150066, Recovered from https://doi.org/10.1038/sdata.2015.66

Gomáriz, F., & Sarría, F. (2018). Efecto de la subdivisión de cuencas y la estimación de variables climáticas en la simulación hidrológica con el modelo SWAT en cuencas semiáridas mediterráneas. *Papeles de Geografía*, (64), 114-113. Recovered from http://dx.doi.org/10.6018/geografia/2018/331531

González-Celada, G., Ríos, N., Benegas-Negri, L., & Argotty-Benavides, F. (2021). Impacto del cambio climático y cambio de uso/cobertura de la tierra en la respuesta hidrológica y erosión hídrica en la subcuenca del río Quiscab. *Tecnología y ciencias del agua*, 12(6), 363-421. DOI: 10.24850/j-tyca-2021-06-09

Guabloche, J., & Saldarriaga, M. (2013). Aspectos económicos y sociales de la región Junín. *Revista Moneda, Banco Central de Reserva del Perú*, 155, 2-17. Recovered from https://www.bcrp.gob.pe/docs/Publicaciones/Revista-Moneda/moneda-155/moneda-155-02.pdf

Gupta, H. V., Sorooshian, S., & Yapo, P. O. (1999). Status of automatic calibration for hydrologic models: Comparison with multilevel expert calibration. *Journal of Hydrologic Engineering*, 4(2), 135-143. Recovered from https://doi.org/10.1061/(asce)1084-0699(1999)4:2(135)

IGP, Instituto Geofísico del Perú. (2005). Diagnóstico de la cuenca del Mantaro bajo la visión del cambio climático. Serie: evaluación local integrada de cambio climático para la cuenca del río Mantaro, vol. 2. Lima, Perú: Fondo Editorial del Consejo Nacional del Ambiente-Consejo Nacional del Ambiente. Recovered from https://repositorio.igp.gob.pe/handle/20.500.12816/715

Lavado, W., & Espinoza, J. C. (2014). Entendiendo los impactos de diferentes tipos de El Niño y La Niña en las lluvias del Perú. *Boletín técnico: Generación de modelos climáticos para el pronóstico de la ocurrencia del Fenómeno El Niño, Instituto Geofísico del Perú*, 1 (3), 4-7. Recovered from https://repositorio.igp.gob.pe/handle/20.500.12816/5043

Lujano, E., Hidalgo, L. S., Diaz, R., Tapia, B., & Lujano, A. (2016). Cambios proyectados de los recursos hídricos bajo escenarios de emisiones RCP 4.5 y 8.5 de modelos climáticos globales del CMIP5 en el Altiplano Peruano. *Revista de Investigaciones Altoandinas - Journal of High Andean Research*, 18(2), 195-204. Recovered from https://doi.org/10.18271/ria.2016.200

Llauca, H., Lavado-Casimiro, W., Montesinos, C., Santini, W., & Rau, P. (2021). PISCO_HyM_GR2M: A model of monthly water balance in Peru (1981–2020). *Water*, 13, 1048, Recovered from https://doi.org/10.3390/w13081048

MINAM, Ministerio del Ambiente. (2015). *Mapa de zonificación ecológica económica del departamento de Junín. Sistema Nacional de Información Ambiental-SINIA*. Recovered from http://geoservidor.minam.gob.pe/zee-aprobadas/junin/

Molina-Navarro, E., Hallack-Alegría, M., Martínez-Pérez, S., Ramírez-Hernández, J., Mungaray-Moctezuma, A., & Sastre-Merlín, A. (2016). Hydrological modeling and climate change impacts in an agricultural semiarid region. Case study: Guadalupe River basin, Mexico. *Agricultural Water Management*, 175(SI1), 29-42. Recovered from https://doi.org/10.1016/j.agwat.2015.10.029

Moriasi, D. N., Arnold, J., Van Liew, M., Bingner, R. L., Hermel, R. D., & Veith, T. L. (2007). Model evaluation guidelines for systematic quantification of accuracy in watershed simulations. *Transactions of the ASAE*, 50, 885-900. Recovered from DOI: 10.13031/2013.23153

Nash, J. E., & Sutcliffe, J. V. (1970). River flow forecasting through conceptual models part I — A discussion of principles. *Journal of Hydrology*, 10(3), 282-290. Recovered from https://doi.org/10.1016/0022-1694(70)90255-6

Nazari, M., Masoud, T., & Karakouzian, M. (2020). Análisis de sensibilidad de la resolución DEM y parámetros efectivos de rendimiento de escorrentía en el modelo SWAT: un estudio de caso. *Revista de Suministro de Agua: Investigación y Tecnología-Aqua*, 69(1), 39-54. Recovered from https://doi.org/10.2166/aqua.2019.044

Neitsch, S., Arnold, J., Kiniry, J., Williams, J., & King, K. (2005). *Soil and water assessment tool theoretical documentation*. Texas, USA: Agricultural Research Service. Recovered from https://swat.tamu.edu/media/1292/SWAT2005theory.pdf

Ocampo, O., & Vélez, J. (2013). Análisis comparativo de modelos hidrológicos de simulación continua en cuencas de alta montaña: caso del río Chinchiná. *Revista Ingenierías Universidad de Medellín, Colombia*. DOI: https://doi.org/10.22395/rium.v13n24a3

OMM, Organización Meteorológica Mundial. (2017). *Directrices de la Organización Meteorológica Mundial sobre la generación de un conjunto definido de productos nacionales de vigilancia del clima*. (N° 1204). Ginebra, Suiza: Organización Meteorológica Mundial.

PDC, Plan de Desarrollo Concertado. (2013). *Plan de Desarrollo Concertado del distrito San Pedro de Saño-Huancayo*. Recovered from https://es.scribd.com/document/294120690/PDC-SANO-2013-2021

Penalba, O., & Pántano, V. (2019). Proyecciones de los flujos de agua en el suelo a partir de los modelos climáticos globales del CMIP5 en Sudamérica y su impacto regional. *Revista Argentina de Agrometeorología*. Recovered from https://www.siteaada.org/_files/ugd/cf1a17_db661b62ac7e4910b830787e59313cea.pdf?index=true

Pilares, I. (2018). *Disponibilidades hídricas reguladas del reservorio Lagunillas y Río Verde para usos múltiples en la cuenca del río Cabanillas* (tesis de doctorado). Universidad Nacional Agraria La Molina, Lima, Perú. Recovered from http://repositorio.lamolina.edu.pe/handle/UNALM/3675

Ramírez, J., & Jarvis, A. (2010). Downscaling global circulation model outputs: The delta method decision and policy analysis working paper No. 1. *International Center for Tropical Agriculture*, 1, 1-18. Recovered from https://cgspace.cgiar.org/handle/10568/90731

Sabino, E., Lavado, W., & Aybar, C. (2019). *Estimación de las zonas de vida de Holdridge en el Perú*. Servicio Nacional de Meteorología y Climatología del Perú. Recovered from https://www.senamhi.gob.pe/load/file/01401SENA-87.pdf

Salas, M. (2019). *Estimación de la carga de sedimentos en la cuenca del río Pitumarca mediante el uso del modelo SWAT* (tesis de Ingeniero Civil). Pontificia Universidad Católica del Perú, Lima, Perú. Recovered from https://tesis.pucp.edu.pe/repositorio/handle/20.500.12404/16823

Sarricolea, P., & Romero, H. (2015). Variabilidad y cambios climáticos observados y esperados en el Altiplano del norte de Chile. *Revista de Geografía Norte Grande*, 183(62), 169–183. https://doi.org/10.4067/S0718-34022015000300010

SENAMHI, Servicio Nacional de Meteorología e Hidrología del Perú. (2014). *El fenómeno El NIÑO en el Perú*. Recovered from https://www.minam.gob.pe/wp-content/uploads/2014/07/Dossier-El-Ni%C3%B1o-Final_web.pdf

Swain, S. S., Mishra, A., Sahoo, B., & Chatterjee, C. (2020). Water scarcity-risk assessment in data-scarce river basins under decadal climate change using a hydrological modelling approach. *Journal of Hydrology,* 590, 125260. Recovered from https://doi.org/10.1016/j.jhydrol.2020.125260

Taylor, K. E., Stouffer, R. J., & Meehl, G. A. (2012). An overview of CMIP5 and the experiment design. *Bulletin of the American Meteorological Society*, 93, 485-498. Recovered from https://doi.org/10.1175/BAMS-D-11-00094.1

VLIR & UNALM, Vlaamse Interuniversitaire Raad University Development Cooperation & Universidad Nacional Agraria La Molina. (2015). *Actividades claves dentro de la UNALM*. Lima, Perú: Vlaamse Interuniversitaire Raad University Development Cooperation y Universidad Nacional Agraria La Molina.

Wongchuig, S. C., Mello, C. R., & Chou, S. C. (2018). Projections of the impacts of climate change on the water deficit and on the precipitation erosive indexes in Mantaro River Basin, Peru. *Journal of Mountain Science*, 15(2), 264-279. Recovered from https://doi.org/10.1007/s11629-017-4418-8